SPATIAL CHARACTERIZATION OF A CAPACITIVELY COUPLED PLASMA IN ARGON AT LOW PRESSURE WITH DOUBLE LANGMUIR PROBE AND OPTICAL EMISSION SPECTROSCOPY DIAGNOSTICS

C. LAURENT[1], J. LO[1], B. CAILLIER[1], L. THERESE[1] AND P. GUILLOT[1]

[1]Université de Toulouse, CUFR J.F. Champollion, Laboratoire DPHE, 81012, Albi, France
christopher.laurent@univ-jfc.fr

ABSTRACT

This work was performed within the framework of the collaborative program PAUD (Plasma Airborne molecular contamination Ultra Desorption) funded by OSEO and certified by French global competitive clusters Minalogic and Trimatec. The aim is to study and develop new technology bricks for next generation molecular decontamination systems, including plasma solution. Previously, an argon inductively coupled plasma (ICP) generated by a radiofrequency (RF) source in a remote (or downstream) reactor was studied with double Langmuir probe measurements and optical emission spectroscopy (OES) diagnostics [1]. In this paper, a parametric study of a Capacitively Coupled Plasma (CCP) generated by the same RF source will be presented. With the same diagnostic tools, the plasma emission, the electronic temperature and density will be investigated for different operating conditions (gas pressure, gas flow and injected power).

1. INTRODUCTION

Offering highly uniform plasmas with a relatively simple plasma generation configuration, CCP source is widely used both at atmospheric and low pressure.

At high pressure, Dielectric Barrier Discharges (DBD) are employed for several applications such as gas, water and biological treatment with the UV emission and reactive species produced [2-4]. They are also designed for surface modification and thin film deposition in online processes.

In our case, at low pressure, the main application is the microelectronic industry. On one hand, CCP are used for uniformity properties in layer depositions, stripping and cleaning for example [5-7]. On the other hand, for ion implantation and etching applications, CCP so-called RF bias are very important [7-8] because they create a flux of charged particles that reached the sample in a directional manner. Thereby, it is common to associate ICP or microwave source with RF bias in a remote reactor. This process for etching applications is known as reactive ion etching (RIE) [7, 9] allowing straight and clean etching with fast rate. Consequently, CCP sources are of great interest in research and industrial field. The next part concerns our experimental setup and diagnostic methods.

2. EXPERIMENTAL APPARATUS AND DIAGNOSTICS

2.1 EXPERIMENTAL SETUP

Our experimental setup is a downstream reactor (Fig. 1) where the gas is introduced through a cylindrical quartz tube which is connected to the process chamber. Next, the gas pumping is provided by a molecular pump (Adixen ATH 500 M) and backed up by a dry vacuum pump (Adixen ACP 40G) located at the bottom of the chamber (Fig. 1).

During operation, a gas flow (1~300 sccm) is fed and kept constant thanks to an automated valve which regulates as a function of the selected pressure (0.005~1 mbar).

The plasma is generated with a 13.56 MHz CCP source (Sairem GRP 10KE) near to the pumping system, the injected power is up to 1 kW through an automatic matching box (Sairem BAAI80AS) for a minimal reflected power (< 10 %).

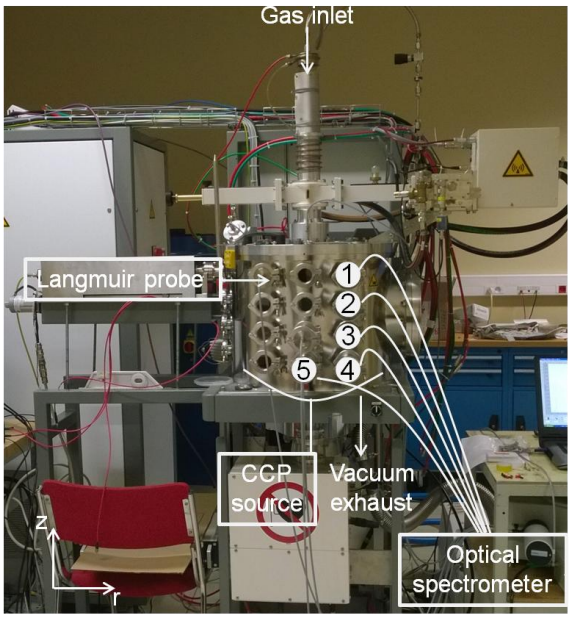

Fig. 1 Experimental apparatus and diagnostics

The reactor is equipped with two portholes with a diameter respectively of 200 and 180 mm through which imaging can be performed. Designed for diagnostics, there are also eighteen KF 40 connections: twelve at the front, four at the left and two on the top of reactor.

2.2 LANGMUIR PROBE

Spatially resolved Langmuir probe diagnostic was performed with an ALP Impedans Automated Linear Drive System (Impedans Ltd, Dublin, Ireland). The cylindrical probe tip (tungsten wire 195 µm in radius and 13 mm in length) is located at 50 mm vertically from the tube end (Fig. 1). The stepper motor allows measurement inside the downstream plasma chamber at different radial positions from r = 0 mm (tube axis) to r = 150 mm (edge of the reactor). An identical wire tip parallel to the current collecting one serves as a reference electrode. The reference probe is used to compensate low frequency shift in the plasma potential.

The plasma potential V_p is obtained from the maximum of the first derivative $I'(V)$. The probe current I_{e0} measured at the plasma potential corresponds to the electron saturation current, and is used to calculate the electron density n_e in the plasma:

$$n_e = \frac{I_{e0}}{A_p}\sqrt{2\pi\frac{m_e}{e^2 kT_e}}$$

where A_p denotes probe surface, e the elementary charge, m_e the electron mass, k the Boltzmann constant and T_e the electronic temperature. In order to obtain the electronic density, $T_{eV} = kT_e/e$ is calculated with the following equation:

$$T_{eV} = \frac{\int_{V_f}^{V_p} IdV}{I_{e0}}$$

where V_f is the floating potential and V_p the plasma potential. Under a Maxwellian distribution assumption where the current measured may be written as:

$$I \approx I_e = I_{e0}\exp\left(e\frac{V-V_p}{kT_e}\right)$$

the integral calculation provides a robust method for the electronic temperature estimation. In terms of numerical resolution, this method is far less hazardous than finding the *ln(I)-V* plot's slope value. Furthermore, the error is introduced mainly by the term:

$$\Delta T_{eV} = \exp\left(-\frac{\Delta U}{T_{eV}}\right)$$

with $\Delta U=|V_p-V_f|$. This term becomes quickly negligible with the ratio $\Delta U/T_{eV}$ increase. In our case where the ratio varies from 2 to 4, the error varies from 2 % to 15 %.

2.3 OPTICAL EMISSION SPECTROSCOPY

The plasma optical emission diagnostic is performed with a Fully Automated Imaging Spectrometer (Horiba Jobin Yvon iHR320). With a grating of 1200 grooves/mm and a focal length of 320 mm, a resolution of 0.06 nm is achieved. Simultaneous spectral acquisitions are carried out at five different locations for spatial distribution characterization thanks to five 200 µm optical fibers joined in a cylindrical tip. Each optical fiber extremity is numbered as shown on figure 1. The emission across the chamber is observed via a collimating lens and a vacuum feedthrough. In this work, the exposure time was set to 3 s with a 50 µm entrance slit-width and the optical emission relative intensity was calibrated using a tungsten halogen light source (LS-1-CAL-220, Ocean Optics Inc.) for the wavelengths of interest varying from 700 nm to 900 nm.

Here, we will consider a photon flux of an *(i)→(j)* transition where *(i)* level can be populated by electron impact from ground state or metastable levels. A general equation can be given by:

$$\Phi_{ij}^{Obs} = n_e\, n_0 \int_0^{\infty} \sigma_{ij}^{Opt}(E)\, f(T_e, E) \sqrt{\frac{2E}{m_e}}\, dE$$

$$+ n_e\, n_{ij}^{*} \int_0^{\infty} \sigma_{ij}^{*}(E)\, f(T_e, E) \sqrt{\frac{2E}{m_e}}\, dE$$

where Φ^{Obs} is the observed photon flux, n_0 and n^* respectively the neutral and the metastable density, σ^{Opt} and σ^* respectively the cross sections from ground state and metastable levels, $f(T_e, E)$ the electron energy distribution function (EEDF) and E the kinetic energy.

According to the cross sections by electron impact from the ground state and the metastable levels which corresponding to these emissions [10], the following approximations of the equation can be done:

$$\Phi_{750.4}^{Obs} = n_e\, n_0 \int_0^{\infty} \sigma_{gs\to 2p_1}^{Opt}(E)\, f(T_e, E) \sqrt{\frac{2E}{m_e}}\, dE$$

$$\Phi_{751.5}^{Obs} = n_e\, n_0 \int_0^{\infty} \sigma_{gs\to 2p_5}^{Opt}(E)\, f(T_e, E) \sqrt{\frac{2E}{m_e}}\, dE$$

$$\Phi_{794.8}^{Obs} = n_e\, n_{1s_3}^{*} \int_0^{\infty} \sigma_{1s_3\to 2p_4}^{*}(E)\, f(T_e, E) \sqrt{\frac{2E}{m_e}}\, dE$$

$$\Phi_{811.5}^{Obs} = n_e\, n_{1s_5}^{*} \int_0^{\infty} \sigma_{1s_5\to 2p_9}^{*}(E)\, f(T_e, E) \sqrt{\frac{2E}{m_e}}\, dE$$

Consequently, the evolution of the 750.4 nm and the 751.5 nm emissions gives a qualitative idea principally on T_e and secondarily on n_e. The evolution of the 794.8 nm and the 811.5 nm emissions, at the same T_e and n_e, can be related to the evolution respectively of the $1s_3$ and $1s_5$ metastable state atoms density.

3. PRELIMINARY RESULTS AND DISCUSSION

Measurements were conducted in argon for different discharge conditions:
- gas pressure from 0.005 to 0.5 mbar;
- gas flow from 15 to 200 sccm;
- forward RF power from 50 to 150 W.

Their influences towards the plasma spatial distribution will be fully investigated in this work. However, we will only present in this paper the impact of the gas pressure between the ICP and CCP.

Figure 2 shows the electronic temperature as a function of the radial position for different pressure for the ICP and the CCP. The gas flow was fixed at 100 sccm for the two cases but the injected power was 500 W for the ICP and 100 W for the CCP.

As we can see for the ICP case, T_e decreases slightly with the radial position from approximately 4 eV to 3.5 eV. The pressure does not seem to have significant influence.

Conversely, in the CCP case, T_e increases with the radial position and also with the gas pressure. Furthermore, for the same working pressure and an injected power five times lower, the electronic temperature obtained in the CCP has comparable values with the ICP case.

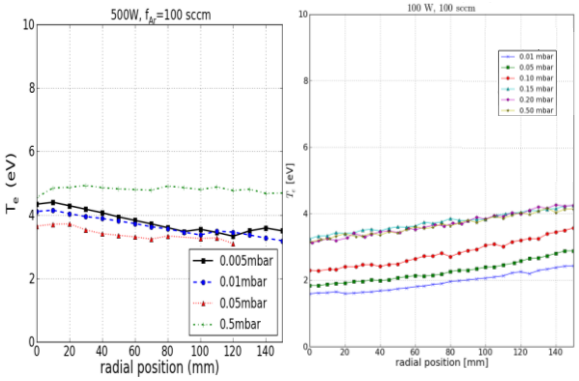

Fig. 2 Electronic temperature in function of radial position for ICP case (left) and CCP case (right)

Figure 3 shows, for the fiber 1, the evolution of four argon emission lines in function of gas pressure for the ICP and the CCP. The same operating conditions as above were applied and the fiber 1 was placed at 120 mm from the tube axis.

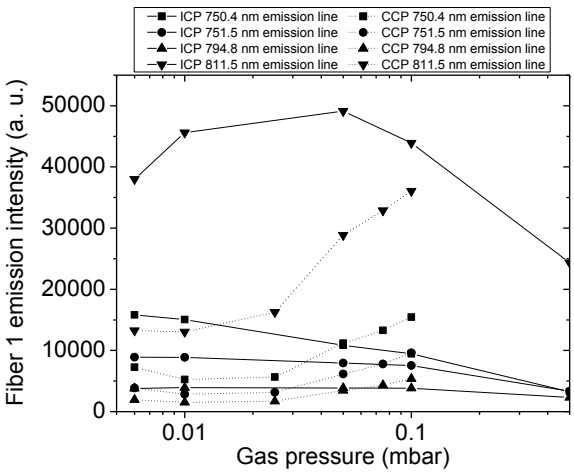

Fig. 3 Optical emission intensity for optical fiber no. 1 for ICP case (solid line) and CCP case (dotted line)

In the first place, for the ICP case, the 750.4 nm and the 751.5 nm emissions decrease with the gas pressure. These variations mean that T_e tends to decrease. In opposite, the 794.8 nm and the 811.5 nm emissions increase so the metastable densities increase too. This result has been already observed on previous work [11] with the line-ratio method. Next, for the CCP, the growth of the 750.4 nm and the 751.5 nm emissions with the pressure signify the increase of T_e. Simultaneously, the 794.8 nm and the 811.5 nm emissions increase. Therefore, the metastable densities are almost constant.
Finally, T_e is higher for the ICP at low pressure or for the CCP at higher pressure. Metastable atom densities are much higher for the ICP.

4. CONCLUSION

The preliminary experimental results have shown Langmuir probe measurements coupled with OES on an ICP and a CCP. Interesting results on the downstream chamber may be obtained and resolved spatially. By presenting a specific case, we have shown that the ICP source is principally designed for reactive species produced while the CCP source leads to a higher kinetic energy of the charged particles. As a result, it could be interesting to associate two plasma sources as described in the introduction. During the conference, more results will be presented as function of all the aforementioned operating conditions.

5. ACKNOWLEDGMENT

The authors wish to express their deep appreciation to all the partners involved in this collaborative program.

REFERENCES

[1] C. Laurent, J. Lo, B. Caillier, L. Therese, P. Guillot, D. Mihailova, G. Hagelaar and P. Belenguer, "Experimental and numerical characterization of an argon RF inductively coupled plasma for surface treatment", IEEE International Conference on Plasma Science (ICOPS), 1-1, 2013.

[2] N. Shimura and R. Ohyama, "Experimental investigation on photochemical NOx gas treatment for diesel engine combustion exhaust by a dielectric barrier discharge type Xe excimer lamp", IEEE Conference on Electrical Insulation and Dielectric Phenomena, 188-191, 2009.

[3] B. Caillier, C. Muja, B. Colin, P. Guillot, J. Dexpert-Ghys and J. M. A. Caiut, "Decontamination of metallic surfaces inocculated with bacillus atrophaeus spores using an UV-C neon-xenon dielectric barrier discharge lamp", IEEE International Conference on Plasma Science (ICOPS), 1-1, 2013.

[4] M. J. Pavlovich, H. W. Chang, Y. Sakiyama, D. S. Clark and D. B. Graves, "Ozone correlates with antibacterial effects from indirect air dielectric barrier discharge treatment of water", Journal of Physics D: Applied Physics, **46**, 145202, 2013.

[5] M. Hiramatsu, K. Shiji, H. Amano and M. Hori, "Fabrication of vertically aligned carbon nanowalls using capacitively coupled plasma-enhanced chemical vapor deposition assisted by hydrogen radical injection", Applied Physics Letters, **84**, 4708-4710, 2004.

[6] H. Y. Chang, Y. S. Lee and K. J. Park, "Advanced plasma sources for the future 450 mm process", 31st International Conference on Phenomena in Ionized Gas, PS2-052, 2013.

[7] K. A. Reinhardt and W. Kern, "Handbook of silicon wafer cleaning technology", William Andrew, 718, 2008.

[8] A. Mitsuo, S. Uchida and T. Aizawa, "Effect of pulse bias voltage and nitrogen pressure on nitrogen distribution in steel substrate by plasma immersion ion implantation of nitrogen", **186**, 196-199, 2004.

[9] L. M. Ephrath, "U.S. Patent No. 4,283,249", Washington, DC: U.S. Patent and Trademark Office, 1981.

[10] J. B. Boffard, G. A. Piech, M. F. Gehrke, L. W. Anderson and C. C. Lin, "Measurement of electron-impact excitation cross sections out of metastable levels of argon and comparison with ground-state excitation", **59**, 2749-2763, 1999.

[11] C. Laurent, J. Lo, B. Caillier, L. Therese and Ph. Guillot, "Spatial characterization of an inductively coupled plasma in argon with optical emission spectroscopy and Langmuir probe diagnostics for surface treatment purpose", 31st International Conference on Phenomena in Ionized Gas, PS3-055, 2013.